Journal of Applied Polymer Science

Preparation and properties of porous polytetrafluoroethylene hollow fiber membrane through mechanical operations

Guochang Liu,[1,2] Congjie Gao,[1] Xiaoming Li,[2] Chungang Guo,[2] Ying Chen,[2] Jinglie Lv[2]

[1]College of Chemistry and Chemical Engineering, Ocean University of China, Qingdao, 266100, China

[2]Lab of Membrane Science and Technology, The Institute of Seawater Desalination and Multipurpose Utilization, State Oceanic Administration, Tianjin, 300192, China

Correspondence to: G. Liu (E-mail: liuguochang_001@163.com)

ABSTRACT: Porous polytetrafluoroethylene (PTFE) hollow fiber membranes were prepared from fine powder through a series of mechanical operations including paste extrusion, heat treatment, stretching and sintering. In contrast to conventional process, the heat treatment used in this study was performed at 200°C to 330°C (near the melting point) on the PTFE nascent hollow fiber (precursor of membrane). The results showed that the introduction of heat treatment step effectively improved the mechanical properties of precursors, the ultimate stress and strain increased observably with heat treatment temperature, which was beneficial to subsequently stretching precursors to make them porous. Furthermore, the morphological changes and improvement of membrane properties caused by stretching operation were investigated for porous PTFE hollow fiber membrane having finer pore size and higher porosity. The porous microstructure of nodes interconnected by fibrils varied depending on the stretching conditions, such as the stretching temperature, rate, and ratio. © 2015 Wiley Periodicals, Inc. J. Appl. Polym. Sci. **2015**, *132*, 42696.

KEYWORDS: extrusion; manufacturing; membranes; morphology; properties and characterization

Received 31 December 2014; accepted 4 July 2015

DOI: 10.1002/app.42696

INTRODUCTION

As is well known, Polytetrafluoroethylene (PTFE) porous membrane has many favorable qualities, including outstanding chemical stability, heat resistance, strong hydrophobicity, and high fracture toughness.[1] These properties make it ideally suited for a variety of liquid and gas separation application, especially for membrane distillation (MD), osmotic distillation (OD), and gas–liquid absorption and stripping application in the strong acid, alkali, high temperature, or corrosive condition.[2–4]

On the other hand, these superior properties are indicative of the difficulty of processing the PTFE resins. In other words, it is impossible to fabricate porous PTFE membrane by common phase inversion or melt spinning methods, particularly the porous hollow fiber membrane.[5–8] Nowadays, the noteworthy methods for fabricating PTFE hollow fiber membrane are emulsion spinning technology or paste extrusion and stretching technology.

The process of emulsion spinning for making PTFE hollow fiber membrane involves blending PTFE emulsion and fiber-forming polymer to get spinning dope, then the dope is spun into hollow fiber by conventional dry-wet spinning method, finally heat-treating and removing the fiber-forming polymer to form porous. Kawai[9] in Japan provided the method and porous PTFE hollow fiber membrane with pores of 0.3–2.0 μm, porosity of about 40%. Huang[10–12] in China did much works on PTFE hollow fiber membrane (porosity 38.6%, water contact angle 134.68°) to reduce the addition of fiber-forming polymer and obtain the porous microstructure of interfacial microvoid. As a result of above studies about emulsion spinning, it is found that the membrane product suffers from inferior porosity and permeability performance.

Commercially, series of porous PTFE membranes have been investigated extensively via paste extrusion and stretching processes by a number of groups. Gore and Associates in USA has done the outstanding works on PTFE flat-sheet membranes used in many areas, such as filtration, fabric, and medical processing applications.[13–19] The Sumitomo in Japan has done much works both on PTFE flat-sheet and hollow fiber membranes.[20–24] Especially the hollow fiber membrane product Poreflon® has been successfully used in membrane bio-reactor for wastewater treatment.[25,26] Moreover, the product Poreflon® is hydrophilic asymmetric membrane having unhomogeneous porous microstructure, the PTFE flat-sheet tape is wrapped on the surface to realize smaller pore size as well as higher porosity.[27] Recently, Markel in USA provides product ECLIPSE

Table I. Specifications of the PTFE Fine Powder Resin

Particle diameter (μm)	Bulk density (g·cm^3)	Reduction ratio	Extrusion pressure (Mpa)	
400-650	0.5	300-1500	RR = 1500	55

Membranes® which relates to porous PTFE hollow fiber membrane used for contacting and separation.[28] The porosity is up to 65%, pore size ranges from 0.005 to 20 microns. Except for patents, there is few detail reports about the ECLIPSE Membranes®. Guo *et al.*[29–31] in China fabricated hydrophobic PTFE hollow fiber membranes (porosity 63.4%, mean pore size 0.46 μm) for MD. In the article, the effect of stretching ratio on the property of membrane was studied. The above results revealed that increasing stretching ratio was positive for pore size and porosity but negative for permeation and mechanical property. However, few reports could be seen about the structural control of porous morphology systematically via a mechanical operation.

This article aims to provide a convenient and low-cost method to produce porous PTFE hollow fiber membrane based on the paste extrusion and stretching technology. The heat treatment was introduced between extrusion and stretching step to improve the mechanical properties of precursor. The porous microstructure consists of node-fibril network produced by longitudinal stretching process. To obtain membrane having finer pore size and higher porosity, several factors related to the porous microstructure were investigated in the course of the stretching operation, including stretching temperature, rate, and ratio.

EXPERIMENTAL

Materials

PTFE fine powder resin was Polyflon F-205 obtained from Daikin Kogyo. The specifications of the fine powder were reported by the manufacturer as listed in Table I. The lubricant used to prepare the pastes was Solvesso® 100 provided by ExxonMobil, with a distillation range of 165°C to 181°C, density of 0.878 g·cm^{-3} at 15.0°C, and kinematic viscosity of 0.98 mm^2·s^{-1} at 25°C. Both the materials were used as received without any further purification.

Preparation of PTFE Nascent Hollow Fiber

The PTFE nascent hollow fiber (precursor of membrane) was prepared as follows. First, the fine powder was mixed slowly with the appropriate amount of the processing aid to produce a paste of 20 wt % in lubricant. Consequently, the paste was continued to be mixed in a thoroughly sealed rotating jar mill at a speed of 35 rpm for one hour. And the paste was aged for 24 h at 50°C allowing uniform lubricant distribution within the paste and better wetting of the powders. Then the paste was preformed into an annular billet by first placing it into a barrel of diameter equal to 30 mm at room temperature. The load cell moved at a constant speed of 800 mm·min^{-1} until the pressure reached up to 1.35 MPa. The pressure was applied for 100 s to remove the air voids and to produce an annular billet of good dimensional stability. The outer diameter, the inner diameter, and the length of the PTFE annular billet were 30, 16, and 250 mm, respectively. Finally, The billet was placed into the ram extruder and the extruder was run at a speed of 15 mm·min^{-1}, the temperature of 80°C. Figure 1 is a schematic display of paste extrusion. The reduction ratio was 1262. The PTFE nascent hollow fiber with outer diameter 1.0 mm and inner diameter 0.7 mm was obtained through the paste extrusion process. The reduction ratio is defined as the following equation:[32]

$$\text{Reduction ratio} = \frac{d_2^2 - d_1^2}{d_4^2 - d_3^2} = 1262 \quad (1)$$

$d_1 = 16$ mm; $d_2 = 30$ mm; $d_3 = 0.7$ mm; and $d_4 = 1.0$ mm

where d_1 is the inner diameter of the PTFE annular billet, d_2 is the outer diameter of the PTFE annular billet, d_3 is the inner diameter of the PTFE nascent hollow fiber, and d_4 is the outer diameter of the PTFE nascent hollow fiber.

Heat Treatment and Stretching Process

The lubricant was completely vaporized at 100°C. Then the PTFE nascent hollow fibers were heat-treated in a thermostatic oven (Carbolite® LHT6/120) at temperature from 200°C to 330°C for 2 h and then quenched at room temperature. In this work, five kinds of precursors of hollow fiber membranes were obtained and named as P-0, P-200, P-300, P-310, P-320, and P-330, corresponding to five treatment temperature (unheat-treated, 200°C, 300°C, 310°C, 320°C, and 330°C), respectively.

Then the precursors were stretched at temperature, T_s, of 10°C to 300°C to axial direction (the longitudinal direction) by a fixed-length stretching apparatus. In the stretching and sintering processes, the sample was held by clamps to prevent retraction. The processes were both finished in the chamber. The chamber used a forced-convection principle in which hot or cold air was

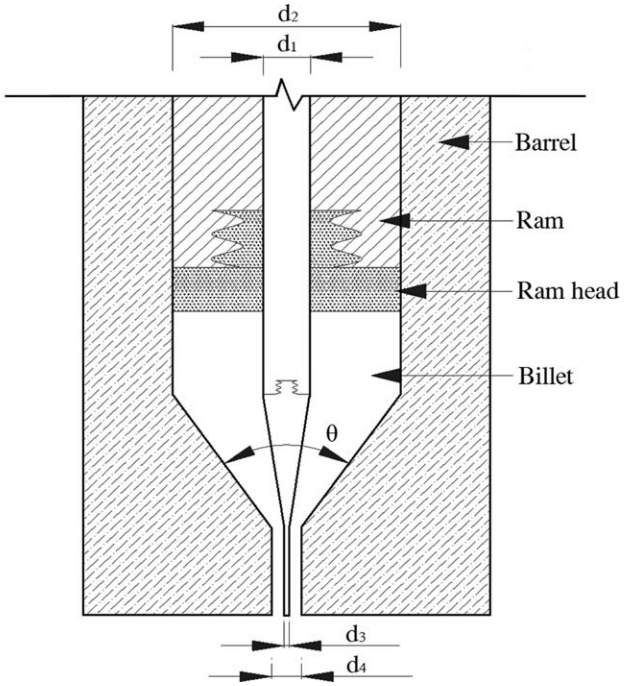

Figure 1. Schematic display of PTFE paste extruder in a longitudinal cross-view.

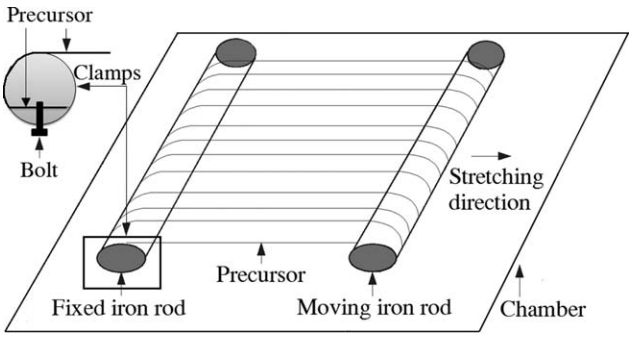

Figure 2. Schematic diagram of stretching system.

recirculated around the specimen. Heating was achieved by passing air over an electrically heated element. Cooling was achieved by integrated cooling device for air. The stretching method is shown in Figure 2. The stretching rate, r_s, was varied from 100 to 3000 mm·min^{-1}, and the stretching ratio, R_s, from 100% to 500%. The stretching ratio, R_s, is defined as equation (2).

$$\text{Stretching ratio} = \left(\frac{L_S}{L_O} - 1\right) 100\% \quad (2)$$

where L_S is the length of the stretched PTFE hollow fiber membrane and L_O is the original length of the precursors before stretched. The original length of precursors, L_O, was 200 mm. After the stretching process, the stretched PTFE hollow fiber membranes were sintered at 340°C for 60 seconds with maintaining the stretched condition in the chamber to ensure membranes strength and dimensional stability. After sintering, the membranes rebound ratio was no more than 2%. The 60 m precursors were stretched to prepare porous membranes for each stretching process. The schematic representation of concept of mechanical operation leading to the formation of PTFE hollow fiber membrane in this study was shown in Figure 3.

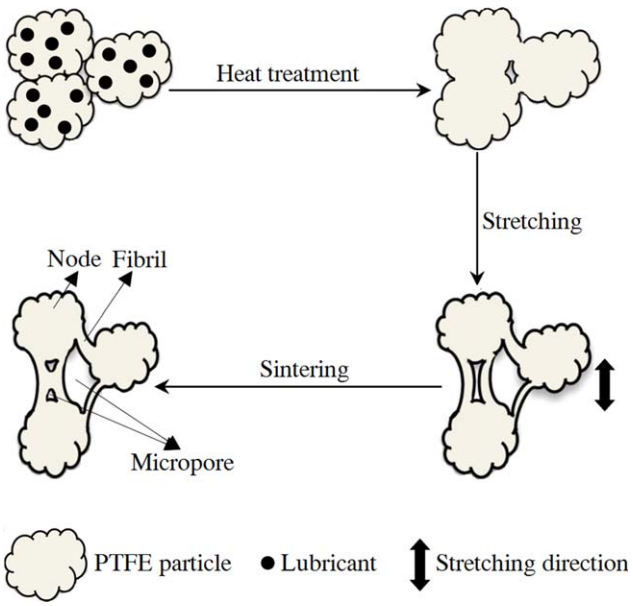

Figure 3. The schematic representation of concept of mechanical operation leading to formation of PTFE hollow fiber membrane. [Color figure can be viewed in the online issue, which is available at wileyonlinelibrary.com.]

Characterization

A differential scanning calorimeter (DSC-200F3 calorimeter, Netzsch, Germany) was used to analyze the thermal behavior of precursors, with the heating rate of 20°C·min^{-1} from 0°C to 400°C. About 10 mg sample was used for each DSC measurement.

The mechanical properties of the precursors, the original length of which was 100 mm, were investigated by measurements with an Instron apparatus (Instron 5965 U1570-500N, Environmental Chambers 3119-609, Instron Corporation, USA) at 25°C and 65% RH. For the breaking strength and elongation at break, the sample was clamped at both ends and pulled in tension at a constant elongation rate of 1000 mm·min^{-1}, five specimens were tested for each sample. Meanwhile, radial compressive resistance performance tests were accomplished also by Instron apparatus with 50 mm compression platen. The testing setup is shown in Figure 4. As discussed later, the tensile and compressive properties of precursors provide useful insight into orientation dependence of crack behavior in stretching process.

The morphological property of the PTFE hollow fiber membrane was studied in terms of field emission scanning electron microscopy (FESEM) (S4800, HITACHIE, Japan) on inner surface. The hollow fiber membranes were sputtered with platinum for 50 seconds using an ion sputtering device (EM ACE200, Leica, Germany) for FESEM observation. The FESEM images were taken at 5 kV.

The porosity and average pore diameter of membrane were characterized by mercury intrusion method using Automatic Mercury Porosimeter (AutoPore IV9500, Micromeritics, USA). For each sample, three specimens were run and taken the average. The pore diameter was carried out by the Washburn's equation, which assumed that the pore or capillary was cylindrical with a circular opening.

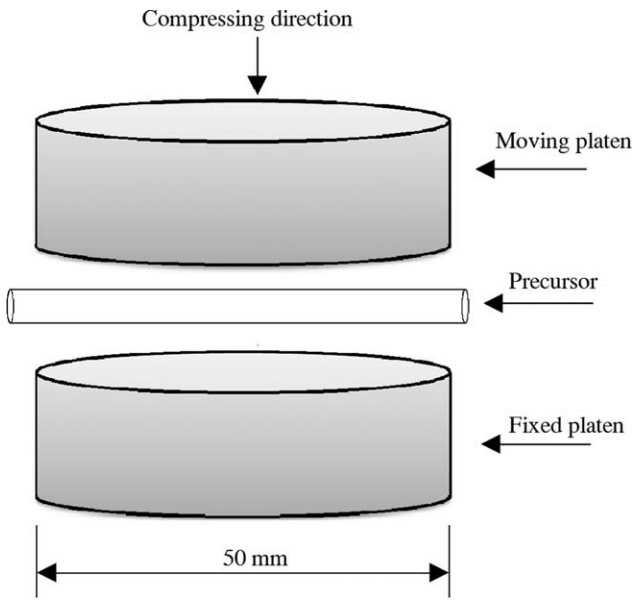

Figure 4. Schematic diagram of compressive failure tests for precursor.

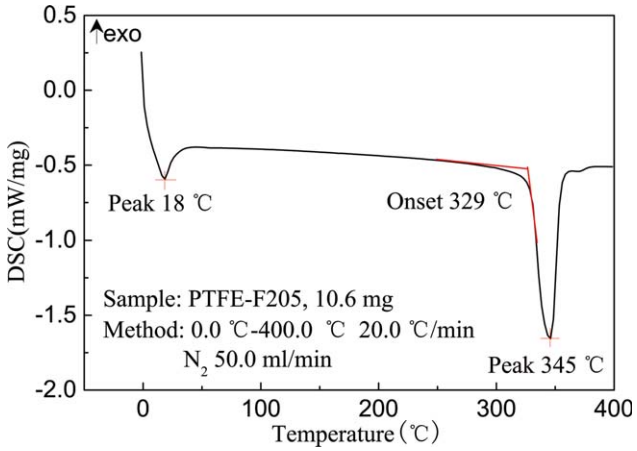

Figure 5. DSC thermogram for precursor P-0. [Color figure can be viewed in the online issue, which is available at wileyonlinelibrary.com.]

The outer diameter and wall thickness of the PTFE hollow fiber membrane was tested by the Leica DM2500M microscope.

RESULTS AND DISCUSSION

DSC Measurement for Determination of the Heat Treatment Temperature

The heat treatment temperature was determined by the DSC data. The thermogram for precursor obtained by DSC analyzer was shown in Figure 5. It could be seen that there were two endothermic peaks near 18°C and 345°C, respectively, in heating process. The peak at 18°C corresponded to the crystalline structure transitions between triclinic crystal and hexagonal crystal.[33] In the transitions, helical conformation transformed from a well-ordered triclinic structure with 13 atoms/180° to a partially ordered hexagonal phase with 15 atoms/turn. The peak at 345°C corresponded to melting peak temperature. The onset temperature was 329°C, which was melting point of PTFE. And, mechanical relaxation of PTFE rigid amorphous fraction produced at temperature of 116°C.[34] Yang *et al.* have demonstrated that the heat treatment could result in merger of neighboring nascent particles along with diffusion of individual molecules, the banded structures unchanged in ellipsoidal nascent particles with suitable time and temperature.[35] However, it was necessary to control the temperature in order to restrict the coarseness of precursor. So in this study, the temperature of heat treatment was chosen from 200°C to 330°C.

Effects of Heat Treatment on Precursor

Mechanical Properties of Precursor. Figure 6 showed the tensile properties (a) and compressive properties (b) of the precursors obtained from different heat treatment temperature. As for P-0 precursor, the elongation at break was 302.58% in tension, maximum load was 9.7 N in compression, which corresponded to the following characters: the precursor was very brittle and more easily broken by slight exterior force. When the heat treatment proceeded on PTFE precursors, the stress and strain were improved significantly except P-200. With heat treatment temperature rising, the stress in tension and the load in compression increased obviously. Meanwhile, as for P-320 precursor, the elongation at break was obviously higher. However, when the temperature rose to 330°C, the elongation at break of precursor decreased to 505.92% as shown in Figure 6(a). All of these tendencies implied that the heat treatment improved the mechanical properties of precursors effectively, which was beneficial to subsequently stretching precursors to make them porous.

Furthermore, as shown in Figure 6(a), the elongated length within the elastic region was around 20%, from 20% to 300–800% extension undergo a plastic deformation processes. As polypropylene and poly(vinylidene fluoride) porous membrane fabricated by stretching processes, the porous microstructure of PTFE hollow fiber membrane appeared in the plastic deformation process.[36,37] So the heat treatment step was beneficial to subsequently stretching precursors to make them porous effectively.

Morphologies of Hollow Fiber Membranes. Figure 7 showed the FESEM images of the stretched PTFE hollow fiber membranes from six precursors at different heat treatment temperature. The stretching was performed at temperature 25°C, with stretching rate, r_S, 1000 mm·min^{-1} and stretching ratio, R_S, 300%.

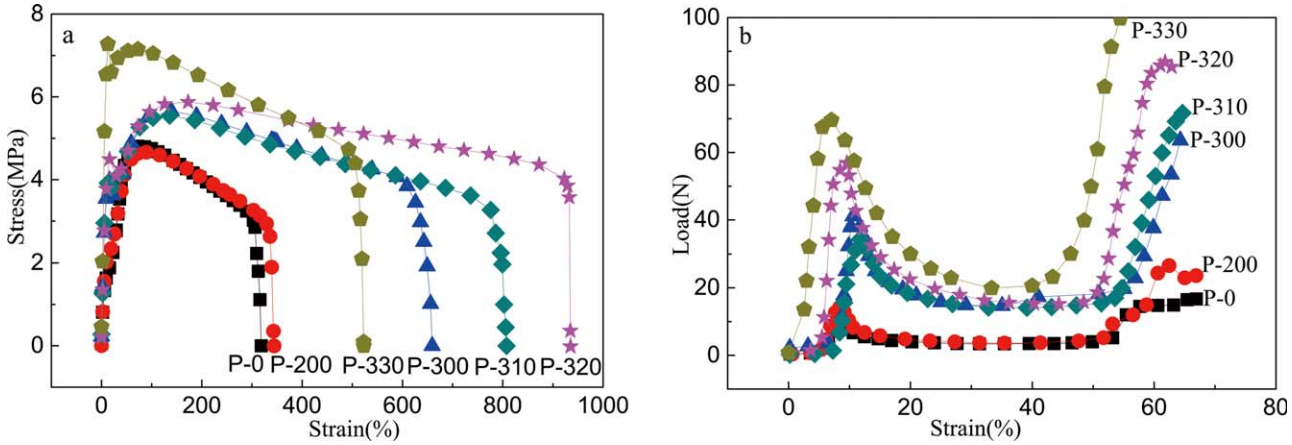

Figure 6. Stress–strain curves of the precursors. (a) tensile properties; (b) compressive properties. [Color figure can be viewed in the online issue, which is available at wileyonlinelibrary.com.]

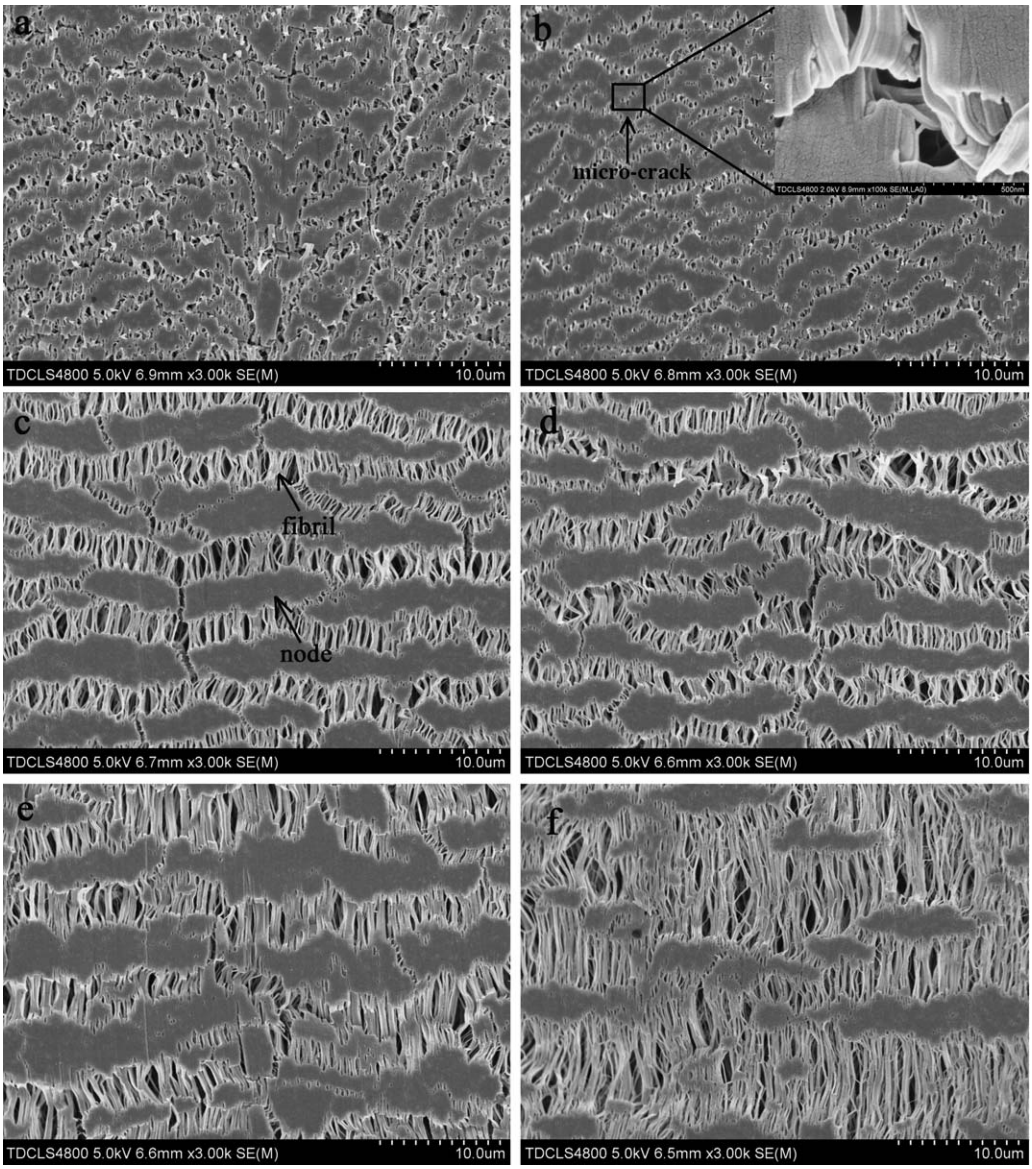

Figure 7. FESEM images of the PTFE hollow fiber membranes fabricated from different heat treated precursors. (a) P-0; (b) P-200; (c) P-300; (d) P-310; (e) P-320; (f) P-330. $T_S = 25°C$, $r_S = 1000$ mm·min^{-1}, $R_S = 300\%$.

It could be seen that all the PTFE hollow fiber membranes have the porous microstructures of nodes interconnected by fibrils. Along with the emergence of microcrack, the shorter length of fibrils formed as shown in Figure 7(b). Although the basic morphology was the same, it could be concluded that the fibrils were elongated and densely distributed parallel to the stretching direction, the amount of nodes decreased as heat treatment temperature increased. It meant that the pore sizes increased with heat treatment temperature. Also it should be noticed that the membranes from unheat-treated and P-200 precursors had much more microcracks, but thin and tiny fibrils, which agreed with their poor mechanical properties as shown in Figure 6. It also meant the fibrils formed between cracks could prevent membrane fracture.[38] Because more fibrils and node linked with one another enabled hollow fiber hardiness in the plastic deformation process, more elongated ratio would be realized.

In summary, the elongation at break and maximum stress/load describing the basic mechanical properties of the precursor can be controlled by varying the heat treatment temperature. Also, the porous microstructure of membranes can be changed by different heat treatment temperature. In the next section, the effect of stretching process on PTFE hollow fiber membrane will be studied from porous microstructure, pore size and porosity.

Effect of Stretching Process on PTFE Hollow Fiber Membrane

Effect of Stretching Temperature. Figure 8 showed the stress–strain curves of precursors P-310 on different stretching temperature. The testing was conducted with stretching rate, r_S, 1000 mm·min^{-1} by the Instron apparatus. Limited by Environmental Chambers, the value of stretching ratio was determined to

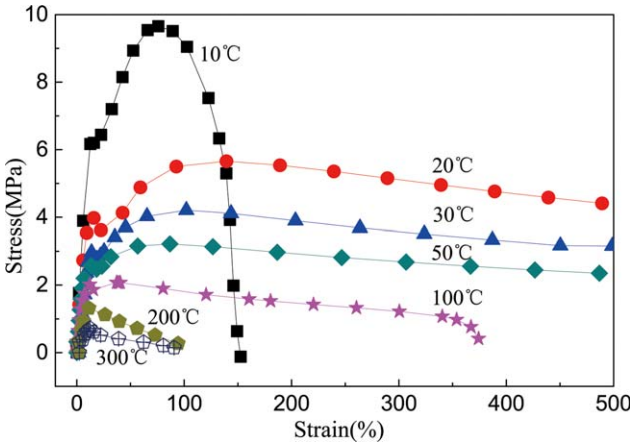

Figure 8. Stress–strain curves of the precursors P-310 on different stretching temperature. [Color figure can be viewed in the online issue, which is available at wileyonlinelibrary.com.]

500%. As shown in Figure 8, the maximum tensile stress of precursors decreased obviously as stretching temperature increased, and elongation at break first increased as temperature increased and then decreased abruptly at higher temperatures (more than 100°C). When the temperature increased to 200°C, the elongation at break of precursors was very low (less than 30%).

For further study, Figure 9 presented the FESEM images of the stretched PTFE hollow fiber membranes to compare the morphological changes among varied stretching temperatures [(a) $T_S = 10$°C, (b) 20°C, (c) 30°C, (d) 50°C, (e) 100°C], with stretching rate, r_S, 1000 mm·min^{-1} and stretching ratio, R_S, 100%.

Remarkable differences were observed on membranes morphologies among the different stretching temperature. The increase in the stretching temperature led to the reduction of the number of cracks per panel image, and consequently, the increase

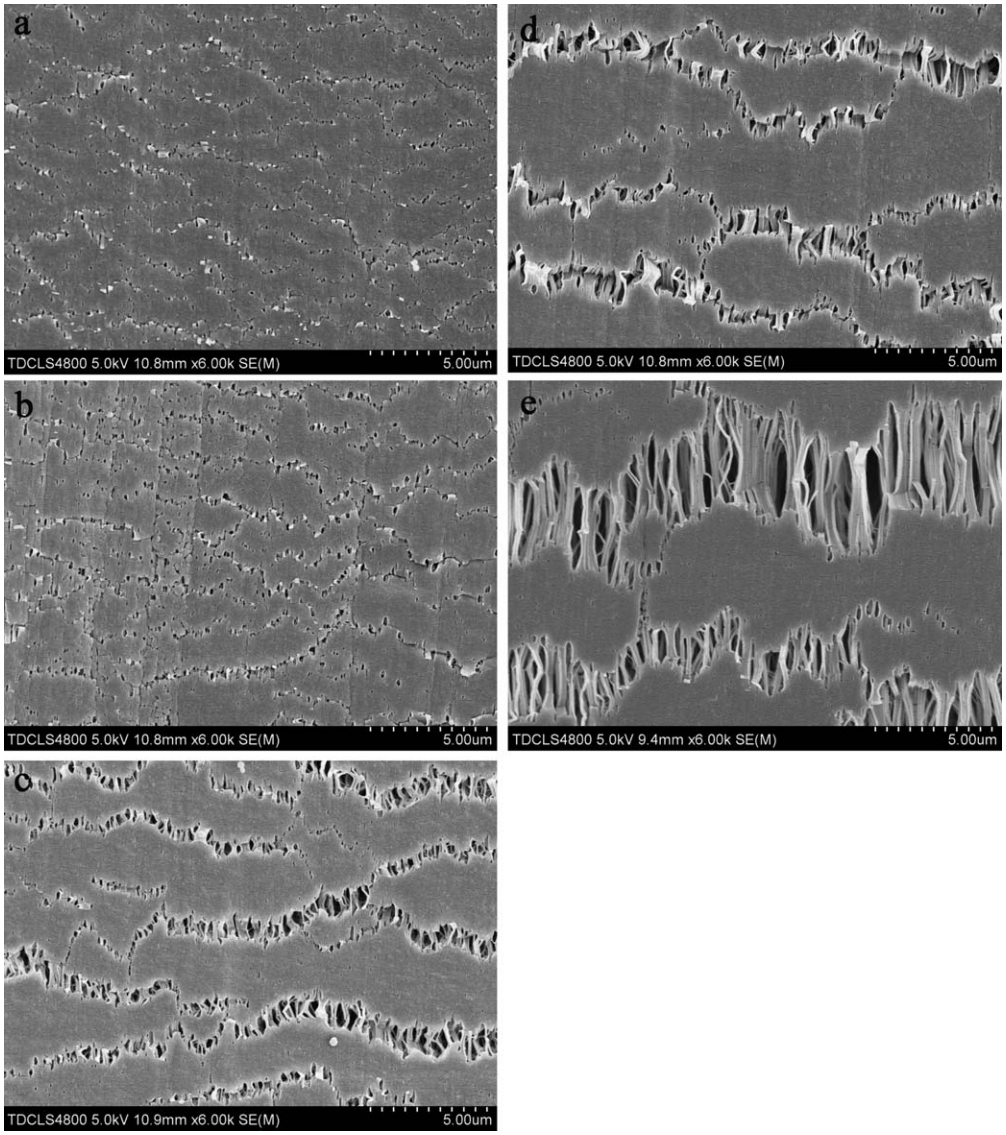

Figure 9. FESEM images of the PTFE hollow fiber membranes showing the effect of stretching temperature on morphology, T_S: (a) 10°C; (b) 20°C; (c) 30°C; (d) 50°C; and (e) 100°C. Precursors P-310, $r_S = 1000$ mm·min^{-1}, $R_S = 100\%$.

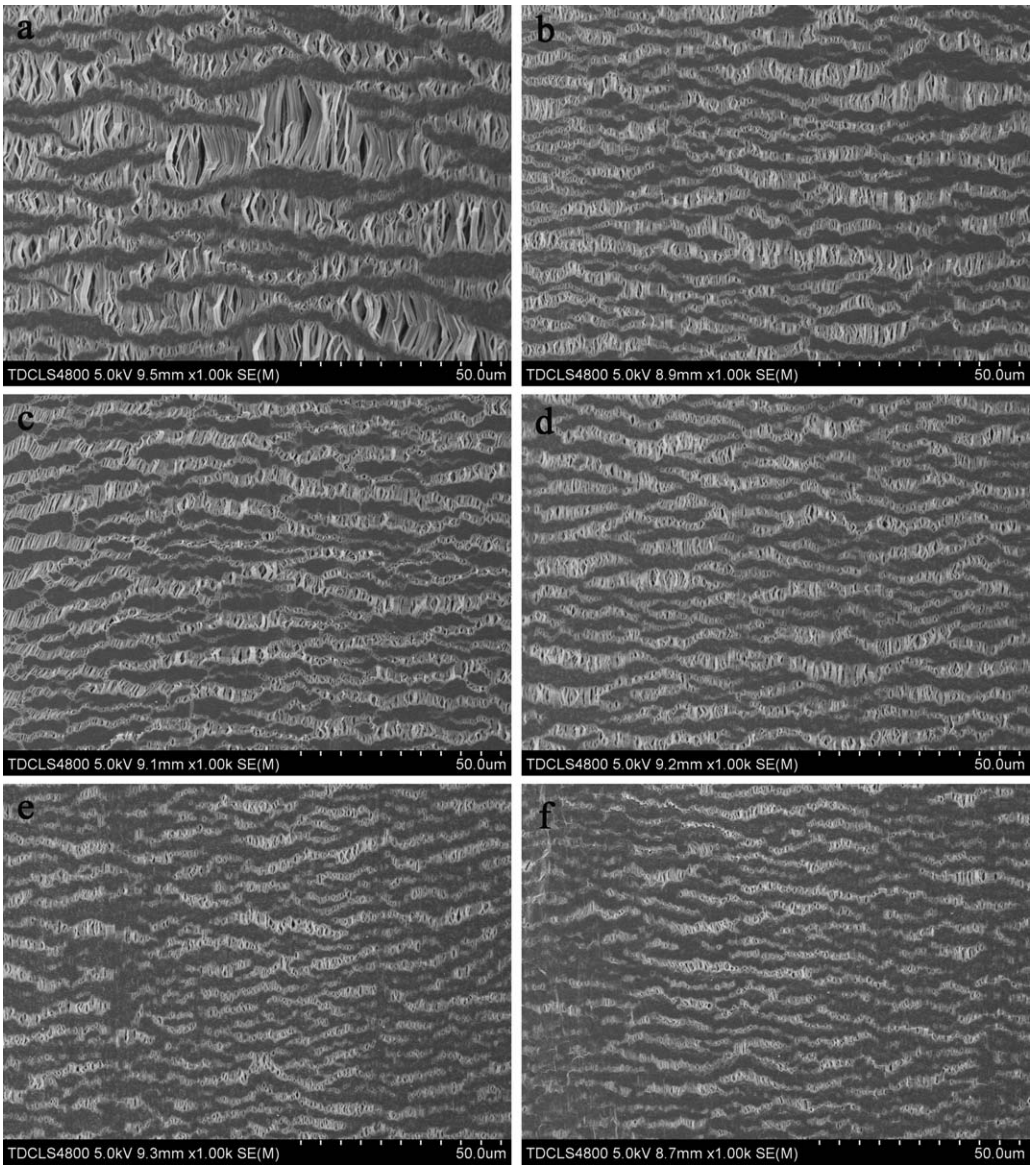

Figure 10. SEM images of PTFE hollow fiber membrane with six different stretching rate, r_s: (a) 100 mm·min^{-1}, (b) 300 mm·min^{-1}, (c) 500 mm·min^{-1}, (d) 1000 mm·min^{-1}, (e) 2000 mm·min^{-1}, (f) 3000 mm·min^{-1}. Precursors P-310, $T_s = 25$°C, $R_s = 200\%$.

length of fibrils and the width of nodes. In other words, pore size of the PTFE hollow fiber membranes increased gradually as stretching temperature increased. This effect suggested it was positive for the formation of the micro-cracks at low T_S, but negative for generation and growth of fibrils. Although higher T_S facilitated growth of fibrils, the number of cracks was few and the R_S of precursors was restricted as shown in Figure 8. So it was difficult to obtain higher porosity at higher or lower T_S. The optimum T_S was from 20°C to 50°C. In the following study, 25°C was adopted as the stretching temperature.

Effect of Stretching Rate. Figure 10 showed the FESEM images of the PTFE hollow fiber membrane obtained at varied stretching rate, r_s, (a) 100 mm·min^{-1}, (b) 300 mm·min^{-1}, (c) 500 mm·min^{-1}, (d) 1000 mm·min^{-1}, (e) 2000 mm·min^{-1}, (f) 3000 mm·min^{-1}, with T_s 25°C R_s 200%. All these FESEM images showed the similar porous microstructure of nodes interconnected by fibrils. The length of fibrils first decreased abruptly with the increase in the stretching rate and became almost constant at a higher stretching rate (more than 300 mm·min^{-1}). This tendency implied that the higher stretching rate facilitates to decrease pore size.

Figure 11 showed the dependence of the porosity on the stretching rate. As shown, membrane porosity increased as the r_s increased in the first, then held steady when r_s increased more than 500 mm·min^{-1}. The value of membrane porosity was 57.5%. The maximum value was 59.19%, which was obtained with r_s 1000 mm·min^{-1}. It revealed that higher porosity obtained at the fast stretching rate. When the r_s was more than 500 mm·min^{-1}, the membrane had finer pore size (Figure 10), which was benefit for maintaining the stabilization of the

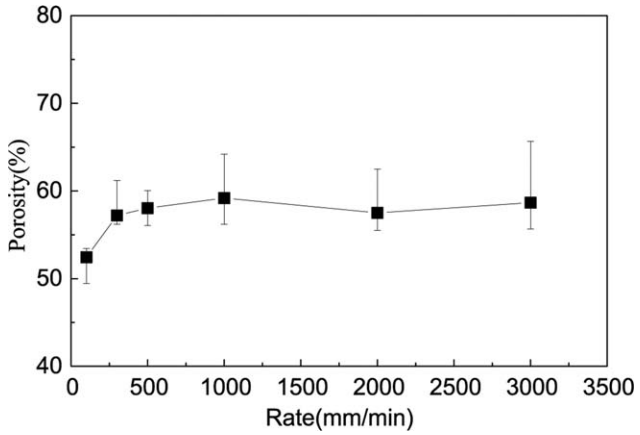

Figure 11. Effects of stretching rate on the porosity of hollow fiber membranes.

membrane structure formed by the stretching operation and could diminish the radial shrinkage of fibrils in the sintering process.

Effect of Stretching Ratio. Figure 12 presented the changes of morphological structure of PTFE hollow fiber membrane with different R_s. It can be learnt that the length of fibrils increased with the R_s increase. As a result, the pore size increased. The effects of stretching ratio on average pore diameter and porosity of PTFE hollow fiber membrane were shown in Table II. When R_s was 100%, the average pore diameter was 0.26 μm, the porosity was 47.24%. When R_s increased to 500%, the average pore diameter was 1.41 μm, the porosity was 78.91%. Therefore, the influence of stretching ratio on the pore size and porosity was very significant to obtain the desired membranes.

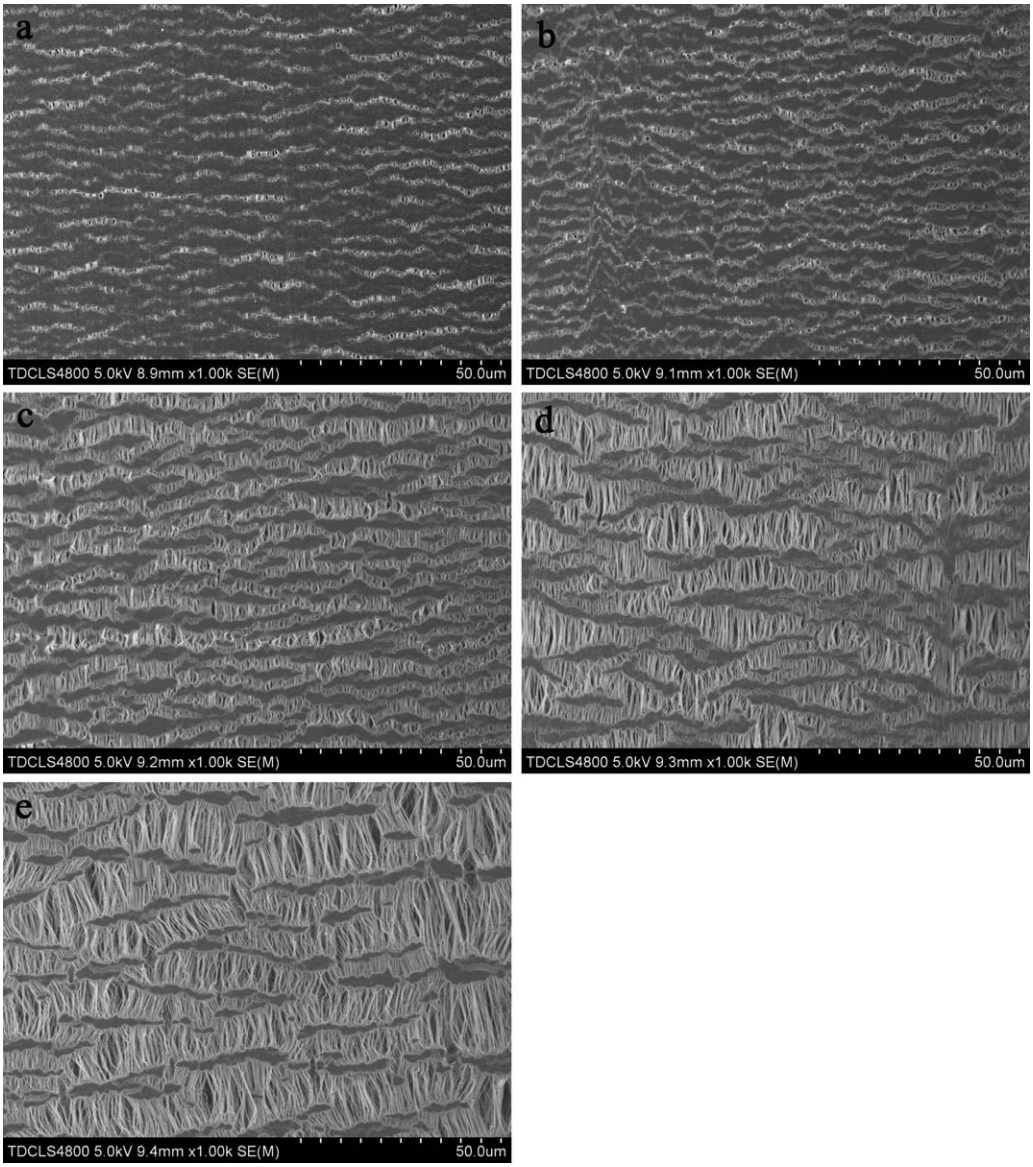

Figure 12. SEM images of PTFE hollow fiber membrane with five different stretching ratio, R_s: (a) 100%, (b) 200%, (c) 300%, (d) 400%,(e) 500%. Precursors P-310, $T_s = 25°C$, $r_s = 1000$ mm·min^{-1}.

Table II. The Characteristics of the PTFE Hollow Fiber Membranes

Membrane ID	0	1	2	3	4	5
R_s (%)	0	100	200	300	400	500
Outer diameter (mm)	1.09	0.88	0.81	0.80	0.81	0.80
Wall thickness (mm)	0.15	0.15	0.14	0.14	0.14	0.14
Average pore diameter (μm)	—	0.26	0.31	0.49	1.14	1.41
Porosity (%)	—	47.24	59.19	65.12	70.31	78.91

Also the outer diameter and wall thickness were listed in Table II. No significant differences in the wall thickness were observed among the PTFE hollow fiber membranes with five stretching ratios compared to precursor. This effect suggests that constant wall thickness corresponded to the formation mechanism of porous microstructure in the PTFE hollow fiber membrane.[39] As polypropylene porous membrane fabricated by stretching processes, the porous microstructure of PTFE hollow fiber membrane appeared in the stretching process. One of the most unique and remarkable developments in the stretching process was the expansion of the precursors in longitudinal stretching direction. The porous microstructure of nodes interconnected by fibrils contributed to the elongation of hollow fiber with wall thickness remained.

Moreover, compared with precursor, the outer diameter of membranes with five stretching ratios decreased obviously, however, the outer diameter of membranes were almost the same when R_s was 200%, 300%, 400%, 500%. This result enabled us to discuss the formation and stabilization of the membrane porous microstructure with the help of sintering process. When the stretched PTFE hollow fibers were sintered at the temperature above the melt point, fibrils pulled out from globular particle would become a fibrous mass, resulting in restraining a fibril from returning to the particulate form. These results were because of the partial melting of PTFE.[40] Meanwhile, it brought about the phenomenon that the PTFE hollow fiber membrane shrink in axial direction (wall thickness). Because of the same sintering temperature and time, the shrinkage degree of membranes with five stretching ratios was almost the same. Also, the shrinkage accounted to the other phenomenon that porosity did not increase two to five fold as R_s after stretching process.

CONCLUSIONS

Polymeric porous hollow fiber membranes were prepared from PTFE fine powder by a series of mechanical operations of extrusion, heat treatment, stretching, and sintering. The PTFE hollow fiber membranes had a highly ordered periodicity characterized by nodes and fibril domains.

The introduction of heat treatment resulted in PTFE nascent hollow fibers with increased mechanical properties, which could prevent them from fracturing or breaking in stretching process. Also, FESEM data showed the pore size of fabricated membranes increased as heat treatment temperature increases. In stretching process, the higher stretching rate resulted in a decrease in pore size and an increase in porosity, the higher stretching ratio resulted in an increase in average pore diameter and porosity.

The data from this study confirmed that this new approach of heat treatment processing was very cost effective for production of PTFE hollow fiber membranes with precisely controlled porous microstructure morphology.

ACKNOWLEDGMENTS

This work was supported by the National Basic Research Program of China for Public Service Institutes: the key technology for preparing hydrophobic PTFE microporous hollow fiber membrane (Grant No. K-JBYWF-2013-T1) and the Key Youth Foundation of State Oceanic Administration (Grant No. 2013502).

REFERENCES

1. Wang, X. Q.; Han, J. C.; Du, S. Y. *Macromol. Symp.* **1999**, *148*, 455.
2. Khayet, M. *Adv. Colloid Interface* **2011**, *164*, 56.
3. Saffarini, R. B.; Mansoor, B.; Thomas, R.; Arafat, H. A. *J. Membr. Sci.* **2013**, *429*, 282.
4. Franco, J. A.; Demontigny, D. D.; Kentish, S. E.; Perera, J. M.; Stevens, G. W. *Ind. Eng. Chem. Res.* **2012**, *51*, 1376.
5. Kang, J. S.; Kim, K. Y.; Lee, Y. M. *J. Appl. Polym. Sci.* **2002**, *86*, 1195.
6. Zryd, J. L.; Burghardt, W. R. *J. Appl. Polym. Sci.* **1995**, *57*, 1525.
7. Chandavasu, C.; Xanthos, M.; Sirkar, K. K.; Gogos, C. G. *Polymer* **2002**, *43*, 781.
8. Sadeghi, F.; Ajji, A.; Carreau, P. J. *J. Membr. Sci.* **2007**, *292*, 62.
9. Kawai, T.; Katsu, T.; Yoshioka, T. U.S. Pat. 5,158,680[P], **1992**.
10. Huang, Q. L.; Xiao, C. F.; Hu, X. Y. *J. Appl. Polym. Sci.* **2012**, *123*, 324.
11. Huang, Q. L.; Xiao, C. F.; Hu, X. Y. *J. Mater. Sci.* **2010**, *45*, 6569.
12. Huang, Q. L.; Xiao, C. F.; Hu, X. Y.; Li, X. F. *Desalination* **2011**, *277*, 187.
13. Gore, R. W. U.S. Pat. 3,953,566[P], **1976**.
14. Yamazaki, E. U.S. Pat. 4,110,392[P], **1978**.
15. Gore, R. W.; Samuel, B A. U.S. Pat. 4,194,041[P], **1980**.
16. Bowman, J. B.; Hubis, D. E.; Lewis, J. D.; Newman, S. C.; Staley, R. A. U.S. Pat. 4,482,516[P], **1984**.

17. House, W. D.; Myers, D. J. U.S. Pat. 4,877,661[P], **1989**.
18. Wang, D. F.; Lick, S.; Alpard, S. K.; Deyo, D. J.; Savage, C.; Duarte, A.; Chambers, S.; Zwischenberger, J. B. *Asaio J.* **2003**, *49*, 564.
19. Haney, A. F.; Hesla, J.; Hurst, B. S.; Kettel, L. M.; Murphy, A. A.; Rock, J. A.; Rowe, G.; Schlaff, W. D. *Fertil. Steril.* **1995**, *63*, 1021.
20. Isamu, S. U.S. Pat. 4,049,589[P], **1977**.
21. Okita, K. U.S. Pat. 4,177,334[P], **1979**.
22. Okita, K. U.S. Pat. 4,248,924[P], **1981**.
23. Akira, H.; Hiroshi, M. U.S. Pat. 5,110,527[P], **1992**.
24. Shinichi, K. J. P. Pat. JP19,920,303,034[P], **1992**.
25. Morita, T.; Kawabe, S.; Okuda, T. J. P. Pat. JP20,100,423, 29A[P], **2010**.
26. Morita, T. U.S. Pat. 2012/103904 A1[P], **2012**.
27. Morita, T. U.S. Pat. 7,735,660 B2[P], **2010**.
28. Hobbs, K. D.; Jerman, R. E.; Wolanski, C. E. U.S. Pat. 2013/075321 A1[P], **2013**.
29. Guo, Y. H.; Chen, J. Y.; Hao, X. M.; Zhang, J. C.; Feng, X. X.; Zhang, H. P. *J. Mater. Sci.* **2007**, *42*, 2081.
30. Zhu, H. L.; Wang, H. J.; Wang, F.; Guo, Y. H.; Zhang, H. P.; Chen, J. Y. *J. Membr. Sci.* **2013**, *446*, 145.
31. Wang, H. J.; Ding, S. B.; Zhu, H. L.; Wang, F.; Guo, Y. H.; Zhang, H. P.; Chen, J. Y. *Sep. Purif. Technol.* **2014**, *126*, 82.
32. Patil, P. D.; Isaias, O.; Christos, S.; Hatzikiriakos, S. G.; Polastri, F.; Kapeliouchko, V. *J. Appl. Polym. Sci.* **2008**, *108*, 1055.
33. Brown, E. N.; Dattelbaum, D. M. *Polymer* **2005**, *46*, 3056.
34. Calleja, G.; Jourdan, A.; Ameduri, B.; Habas, J. P. *Eur. Polym. J.* **2013**, *49*, 2214.
35. Yang, J.; Petersen, K. L.; Williams, R. A.; Geil, P. H.; Long, T. C.; Xu, P. *Chinese J. Polym. Sci.* **2005**, *23*, 123.
36. Sung, W. H.; Seung, M. W.; Deuk, J. K.; O, O. P.; Sang, Y. N. *Macromol Res.* **2014**, *22*, 618.
37. Du, C. H.; Zhu, B. K.; Xu, Y. Y. *Macromol. Mater. Eng.* **2005**, *290*, 786.
38. Dibazar, A. R.; Shokrollahi, P.; Barzin, J.; Rahimi, A. *J. Membr. Sci.* **2014**, *470*, 458.
39. Kitamura, T.; Kurumada, K. I.; Tanigaki, M.; Ohshima, M.; Kanazawa, S. I. *Polym. Eng. Sci.* **1999**, *39*, 2256.
40. Kitamura, T.; Okabe, S.; Tanigaki, M.; Kurumada, K. I.; Ohshima, M.; Kanazawa, S. I. *Polym. Eng. Sci.* **2000**, *40*, 809.